Salt-Induced Control of the Grafting Density in Poly(ethylene glycol) Brush Layers by a Grafting-to Approach

Ortiz, Roberto; Olsen, Stefan; Thormann, Esben

Published in:
Langmuir

Link to article, DOI:
10.1021/acs.langmuir.8b00030

Publication date:
2018

Document Version
Peer reviewed version

Salt-induced control of the grafting density in poly(ethylene glycol) brush layers by a grafting-to approach

Roberto Ortiz,[1,*] Stefan Olsen,[2] Esben Thormann[1,*]

[1] Department of Chemistry, Technical University of Denmark, 2800 Kgs. Lyngby, Denmark

[2] Hempel A/S, 2800 Kgs. Lyngby, Denmark

*Corresponding authors: Roberto Ortiz: Robor@kemi.dtu.dk, Esben Thormann: Esth@kemi.dtu.dk

ABSTRACT

In this work a method to obtain control of the grafting density during the formation of polymer brush layers by the grafting-to method of thiolated polyethylene glycol onto gold is presented. The grafting density of the polymer chains was adjusted by adding Na_2SO_4 in concentrations between 0.2 and 0.9 M to the aqueous polymer solution during the grafting process. The obtained grafting densities ranged from 0.26 to 1.60 chains per nm^2, as determined by surface plasmon resonance. The kinetics of the grafting process were studied in situ by quartz crystal microbalance with dissipation, and a mushroom to brush conformational transition was observed when the polymer was grafted in the presence of Na_2SO_4. The transition from mushroom to brush was only observed for long periods of grafting, highlighting the importance of time to obtain high grafting densities. Finally, the prepared brush layer with the highest grafting density showed high resistance to the adsorption of bovine serum albumin, while layers with a lower grafting density showed only limited resistance.

INTRODUCTION

Polymer layers grafted to a substrate can radically affect interfacial properties, such as wettability, adhesion, friction and biocompatibility.[1-6] An interesting type of layers are polymer brushes, which are thin layers of extended polymer chains where one end of each chain is grafted to a surface.[7] The entropically unfavorable chain extension is a result of excluded volume effects which arise when the separation between the grafted chains is smaller than two times the radius of gyration of the unperturbed polymer chain. This conformational change gives rise to a polymer layer with a high internal pressure and a number of different properties which differs from a layer of unpertubated

polymer chains,[8] and the formation, characterization and stability of such layers is thus of high interest for a variety of scientific fields.[1, 9]

Commonly, the formation of polymer brushes is either achieved using grafting-to or grafting-from approaches. To form densely packed polymer chains, the main factors to overcome are the excluded volume interactions, that is, the hindered access to the surface by the already grafted polymers. The grafting-from approach overcomes this problem by growing the polymers from the surface, e.g., using atom transfer radical polymerization, nitroxide-mediated polymerization or reversible addition-fragmentation chain transfer.[10-13] These methods produce dense brushes with controlled chemical functionality by growing the polymer from an initiator bound to the surface. However, these methods generally also result in poor control of the degree of polymerization and generally require oxygen free conditions. In the grafting-to approach, end-functionalized polymers bind to complementary functional groups located at the surface. This process uses previously characterized polymer chains with known degrees of polymerization and narrow molecular weight distributions, from which a well-defined brush can be constructed with high control of the degree of polymerization, thickness and chemical composition.[14-15] The grafting process will normally be relatively unhindered until a surface covered with close-packed random coils is achieved. Thereafter, steric repulsion between the polymer chains strongly limits the further attachment and thus the formation of a highly extended brush. To overcome this, the grafting conditions can be changed to reduce the excluded volume effect by using polymer melts or polymers in low-solubility conditions.[16-17] The conditions for which the solvent is poor enough that the effects of the excluded volume expansion are cancelled are called θ-solvent conditions. The θ-solvent conditions, where the conformation of each polymer chain is controlled solely by its configurational entropy, can be obtained for an aqueous solution by controlling the ionic strength, the salting-out strength of the salt and the temperature,[14, 18] the choice of a θ-solvent (generally an organic solvent)[19] or by using concentrated homopolymer solutions that reduce the solubility of the polymer.[20] However, only a few studies attempting to control the grafting density using low solubility conditions of the polymers have been reported.[14, 21-25]

Significantly, brushes composed of polyethylene glycol (PEG), a neutral polyether with high water solubility that is non-toxic, well-characterized and has special osmotic and elastic properties when interacting with water,[26] are interesting due to their excellent resistance against protein adsorption, wide range of commercially available molecular weights, low price and ease of end functionalization. Biofilm formation is initiated by the formation of a conditioning film constituted by small organic molecules and proteins present in the water or released by the organisms willing to colonize the

surface.[27] By reducing or avoiding the attachment of these molecules and proteins, the formation of such biofilms can be hindered or slowed down. The growth of biofilms on surfaces that are in contact with water produce important economic losses in a variety of fields and industries, such as biomedicine,[27-31] the marine industry,[27, 32-33] food packaging and processing[27] and water purification membranes.[34] The exact mechanism of PEG-functionalized surfaces to resist non-specific adsorption is still up for debate, but numerous reports show decreased protein adsorption with increasing grafting density and a larger degree of polymerization when the polymer adopts a brush conformation.[18, 21, 24, 35-36] The resistance is thought to depend on the hydrophilic and neutral character of PEG, meaning that it will not form hydrophobic and electrostatic interactions with proteins, and the strong hydrogen binding between PEG and water creates a hydration layer that prevents interactions with proteins.[37-39] On the other hand, it has been shown that PEG can form weak hydrogen bonds with some proteins depending on the temperature, the molecular weight and the grafting density.[40-43] Recent findings show as well that the highest grafting density does not always give the best resistance to fouling in all conditions.[44-45] Then, one of the main challenges that remains is to precisely control the grafting density during the grafting process. To accomplish that, a deeper understanding of the formation of the grafting process is necessary.

Surprisingly, the experimental literature related to the study of grafting kinetics using the grafting-to approach is not exhaustive. Traditionally, two different regimes are described. Firstly, a diffusion-controlled regime, in which the grafting follows a logarithmic trend, can be described by the random sequential adsorption model where the polymer coils adsorb randomly to an interface until there is no more space to accommodate new coils.[46-48] Second, a penetration-limited regime exists in which little grafting is achieved due to the entropic hindrance of the layer formed in the first regime.[49] Meticulous investigations regarding polymer grafting kinetics by Penn and coworkers for different polymer systems encountered a third regime where thermal fluctuations create openings large enough to accommodate new coils, and a mushroom to brush conformational change occurs.[19, 50-58]

In the present work, we demonstrate how the grafting density of the PEG brush layer can be systematically tuned by the addition of a salt (Na_2SO_4) with a strong salting-out effect. The thiolated polymers are directly attached to gold, which is a widely used material in bio-interface science. The grafting density of the polymer is determined from SPR, and the kinetics of the grafting process for the different salt conditions are studied in situ with QCM-D. Finally, the resistance to the adsorption of bovine serum albumin (BSA) is studied for PEG brush layers with low- and high grafting densities.

EXPERIMENTAL SECTION

Materials

The polymer samples were monodisperse, methoxy terminated PEG thiol of M_n = 5000 g mol^{-1} ($M_w/M_n \leq 1.08$; N≈113) with a purity > 95% and a density of 1400 kg L^{-1} purchased from Nanocs (New York, USA). Non-thiolated PEG of M_n = 6000 g mol^{-1} with a density of 1400 kg L^{-1}, Na_2SO_4 and bovine serum albumin (96%) were purchased from Sigma-Aldrich.

The polymer solutions used for grafting experiments were prepared by mixing and vortexing PEG and water or an aqueous solution containing Na_2SO_4 at room temperature for 1 hour. The condition close to the cloud point was selected by visually observing the cloudiness of the solution to find the concentration just before phase separation occurred. Cloudiness was observed for concentrations higher than 0.9 M Na_2SO_4 using 0.6% thiolated PEG (see Fig. S1).

All other reagents were of analytical reagent grade and were used without further purification. Water purified with a Milli-Q apparatus (Millipore, Bedford, MA, U.S.A.) to a specific resistivity (18.2 MΩ cm at 25°C) was used to prepare all aqueous solutions.

Surface Plasmon Resonance (MP-SPR)

SPR sensor slides with a ∼50 nm gold top layer and a ~ 2 nm chromium adhesion layer (BioNavis, Ylöjärvi, Finland) were used for all SPR experiments. All SPR experiments were performed at 22.0°C with an SPR Navi 220A instrument (BioNavis Ltd, Ylöjärvi, Finland) equipped with two light source pairs providing 670 and 785 nm excitation.

The SPR gold sensors slides were cleaned by boiling in NH_3 (30%)/H_2O_2 (30%)/H_2O (1:1:5, v/v) oxidizing solution for 15 minutes. The sensor slides were then rinsed thoroughly with water, blow dried with N_2 and used directly.

PEG was grafted by placing the SPR gold sensor slides in a sealed container with aqueous solutions containing 0.6 mg mL^{-1} thiolated PEG and Na_2SO_4 of different concentrations (ranging from 0 to 0.9 M) under stirring at room temperature for approximately 16 h. Thereafter, the gold sensor slides were thoroughly washed with water and dried with N_2. All experiments were repeated at least in duplicate, and the statistical errors were calculated from the mean of these values.

For the determination of the dry thickness, angular scans were taken for all SPR gold sensor slides in air before and after grafting by waiting for stabilization of the sensor slides on the instrument for 20 minutes. The experimental SPR data were simulated with optical fitting software (Winspall 3.1),[59]

which is based on the Fresnel equations and the recursion formalism. The SPR signal of the pure sensor slide surface was simulated first in order to obtain the background for the subsequent simulation in the desired medium, as previously described.[60] The grafting density was calculated using the thickness values obtained experimentally by SPR. For these calculations, a refractive index of 1.456 and a bulk density 1.09 g cm^{-3} were used for dry PEG.[61]

Quartz Crystal Microbalance with dissipation (QCM-D)

QCM-D data acquisitions were performed using a Q-sense E1 system (Biolin Scientific AB, Gothenburg, Sweden) equipped with a peristaltic pump from Ismatec (Wertheim, Germany). The temperature of the solution in the chamber was maintained at 22.0°C ± 0.02°C and a flow rate of 80 µL min^{-1} was used for all the experiments. The adsorption process was monitored until the QCM-D signal reached a plateau, when changes of frequency were less than 1 Hz for 30 min (taken as equilibrium condition). The AT-cut piezoelectric quartz crystal disks coated with gold used as the sensor chip (Q-sense, Biolin Scientific AB, Gothenburg, Sweden) had a fundamental frequency of 4.95 MHz ± 50 kHz and vibrate in the thickness-shear mode with the overtone *n* of 1, 3, 5, 7, 9, 11 and 13. All experiments were performed at least in triplicate. The data presented here correspond to the change in vibrational frequency and its associated dissipation ($\Delta f_n = \Delta F_n/n$ and ΔD) of the sensor chip vs. time.

The QCM-D sensor chips were first flushed with copious amounts of Milli-Q water and 99.7% ethanol. They were then immersed in a 5:1:1 H_2O:NH_4OH (30%):H_2O_2 (30%) solution at 75°C for 5 minutes, followed by rinsing in copious amounts of water. Finally, the substrates were sonicated in 99.7% ethanol, rinsed with water and blow-dried with nitrogen. The clean sensor chips were mounted directly on the QCM-D instrument.

First, Δf and ΔD were measured in air to evaluate the correct mounting of the sensor chip. Afterward, water was introduced in the cell until a stable baseline of *f* and *D* was observed. An aqueous Na_2SO_4 solution of the same concentration as the one containing the polymers was flushed through the system until a stable baseline was obtained. Then, 0.6 mg mL^{-1} of thiolated PEG in the corresponding aqueous solution was flowed over the surface for 16 hours, and then the cell was washed with the same aqueous Na_2SO_4 solution as used before grafting until a stable baseline was obtained. In a last step, the cell was flushed with water. The measured frequency and dissipation shifts for the fifth overtone was used to evaluate the binding before, during and after adsorption and rinsing.

Bovine serum albumin (BSA) was prepared in a concentration range from 0.01 – 5 mg mL^{-1} in phosphate buffered saline (PBS) pH 7.4. Prior to the injection of BSA, PBS was flushed through the cell until a stable baseline was reached. Each solution of BSA was flowed over the surface for 20 minutes followed by rinsing with PBS for 20 minutes. The measured frequency shift was taken as the values before and after injection of BSA. The amounts of BSA adsorbed onto the surfaces were calculated for the 3rd overtone.

To evaluate the viscoelastic properties of a film and the validity of the Sauerbrey equation for a system, the relationship $\Delta D_n/(-\Delta f_n/n)$ can be used. For values of this ratio well below 4 x 10^{-7} Hz^{-1} for a 5 MHz crystal, the film can be approximated as rigid.[62] PEG films showed higher values than 4 x 10^{-7} Hz^{-1}, and then the films are considered viscoelastic. The mass calculated using the Sauerbrey relation is therefore expected to be an underestimation of the actual mass for these films.

RESULTS AND DISCUSSION

Investigation of PEG grafted onto gold surfaces using SPR and QCM-D

Determination of the amounts of thiolated PEG (5 kDa) grafted to gold coated surfaces in the different aqueous solutions of Na_2SO_4 was performed using angular SPR spectroscopy and QCM-D. These two techniques are fundamentally different in the sense that SPR, as an optical technique, measures the dry mass of the attached polymers, while QCM-D as a resonance technique measures the wet mass of the attached polymers, e.g., the attached polymers and the solvent molecules associated with the polymer layer.

In these experiments, the concentration of Na_2SO_4 was varied from 0 to 0.9 M while the concentration of polymer was kept at 0.6 mg mL^{-1} and the temperature was kept at 22.0°C. For salt concentrations below 0.9 M, clear and homogeneous solutions were obtained, while for salt concentrations above 0.9 M, the solutions became turbid (Fig. S1). This phase separation at concentrations higher than 0.9 M was induced by the strong salting-out effect of SO_4^{-2}, reflected in its placement in the Hofmeister series.[63-64] This also implies that the solvent quality (with respect to PEG) gradually worsens as the concentration of Na_2SO_4 is increased from 0 to 0.9 M.

Using SPR, the amount of covalently attached PEG at the different solubility conditions was calculated using previously reported methods in the literature.[65-66] The SPR gold sensor slides were modified in a container using stirred solutions, and the optical thickness of the polymer films were calculated by fitting the full angle scans for the modified and unmodified slides using a multilayer model. First, the optical properties of the unmodified SPR gold sensor slide were calculated by fitting the SPR full angle scan, measured for the same SPR sensor slide as used later for the attachment of PEG. The obtained optical properties were used as a starting point for finding the optical properties of the grafted PEG layer. Typical SPR curves and fits obtained in air for dry surfaces are shown in Fig. 1(A) for an unmodified gold sensor slide (blue curve), the same surface modified with PEG using water as the solvent (red curve) and a thiolated PEG modified surface using 0.9 M Na_2SO_4 (black curve). As observed, the angular dip in reflectivity for the polymer grafted under low solubility conditions (high salt) shows a bigger shift than when modified under high solubility conditions (no salt) (Fig. 1(B)). The larger shift in the position of the angular dip is related to a larger optical thickness of the polymer layer grafted on the surface. For concentrations of Na_2SO_4 up to 0.6 M, an increased shift in the position of the angular dip was observed for increased concentrations of salt. However, for PEG layers grafted in 0.8 and 0.9 M Na_2SO_4, a smaller shift in the position of the

angular dip was found compared to that for the PEG layer grafted in 0.6 M Na_2SO_4. This is interpreted as a maximum in the thickness and is found for the PEG layer grafted in 0.6 M Na_2SO_4. Finally, the optical thickness obtained for each grafting condition was converted to the dry polymer mass per unit area by multiplying by the polymer density.

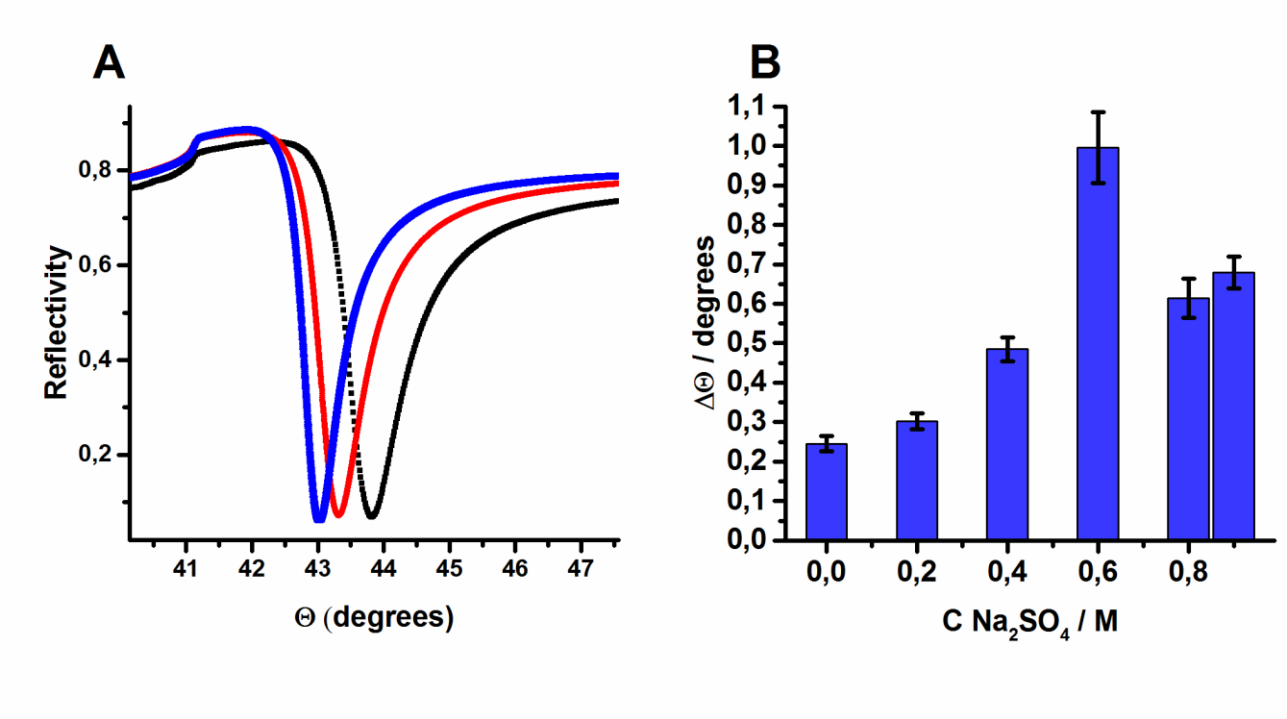

Figure 1. (A) Angular scans and fittings for unmodified SPR gold sensor slides (blue), dry films of PEG grafted when the polymer was dissolved in water (red) and 0.9 M Na_2SO_4 (black) for a wavelength of 670 nm. (B) $\Delta\theta$ of the dip for dry films grafted using aqueous solutions of Na_2SO_4.

To obtain more detailed information about the grafting process and the mass of the hydrated brush layers (including the solvent), QCM-D was used. In a typical experiment, the baseline was firstly obtained in water, and secondly in the aqueous salt solution, where after the polymer in the same aqueous salt solution was injected at a constant flow rate overnight. Then, the aqueous salt solution used for the baseline was injected in order to remove physically adsorbed polymers and finally, the system was rinsed with milli-Q water (Fig. S2). Fig. 2 show the changes in Δf and ΔD as a function of time for the different solvent conditions. From this, one can deduce information about both the grafting kinetics as well as the total attached mass (including the solvent) and the conformation of the grafted PEG layer. The former part will be discussed in a later section, while the total attached mass will be discussed here.

To be able to compare the layers obtained under the different grafting conditions, the changes of Δf and ΔD between the baseline obtained in water and the values obtained after the last rinsing step in water were determined (Fig. 3). By doing so, all the layers were compared in the same (good) solvent condition, and the difference in liquid loading by the different saline solutions was thus eliminated. Typically, a good estimation of the attached amount (and other film properties) can be estimated using the Sauerbrey equation (for rigid films) or the Voigt model (for viscoelastic films).[62] However, although the layers show viscoelastic properties, the viscoelastic model was difficult to fit correctly since the precise hydration level and thus the density of the grafted polymer (which will further change during the grafting process and be different for the different solvent conditions) is difficult to estimate. On the other hand, the Sauerbrey equation applies for calculating the mass of rigid films while it does not take the viscoelastic contribution into consideration. Thus, the mass obtained using the Sauerbrey equation for these non-rigid films is an underestimation of the real mass due to the absence of the viscoelastic contribution in the calculation. However, it can be used as a qualitative measure of the wet mass. The masses calculated using the Sauerbrey equation for all the PEG layers grafted under the different solvent conditions are presented in Table 1. Fig. 2 and 3 also show the result of flowing non-thiolated PEG dissolved in water or in 0.9 M Na_2SO_4 over the QCM-D gold sensor surface. Only a very limited amount of PEG is physically adsorbed under these conditions. This illustrates first that the PEG chains have a weak but measurable interaction with the Au surface and second, that the larger mass measured for thiolated PEG is due to covalent grafting and not just physical attachment.

As Table 1 shows, the wet mass obtained by QCM-D naturally exceeds the dry mass obtained by SPR, and the water content can in principle be determined by the difference between them. The highest water content was found for the PEG layer grafted in pure water (63%), while the apparent water content decreased when the PEG layers were grafted in Na_2SO_4 solutions. This trend most likely reflects the fact that the mass obtained with the Sauerbrey equation is more underestimated the more extended the layer becomes. Taking this into consideration, we consider the water content in all cases to be at least 60%, which is well in line with water contents in the range of 50-90% previously reported for hydrated polymer layers.[67-69]

The dry mass obtained from the SPR measurements shows a maximum when grafted in 0.6 M Na_2SO_4, while the wet masses obtained from the QCM measurements, in contrast, increased up to 0.9 M Na_2SO_4. To explain this apparent discrepancy, one should pay attention to the curves in Fig. 2 showing the attachment of PEG in 0.8 and 0.9 M Na_2SO_4. During the rinsing step (after grafting), at

these two salt concentrations and especially for the attachment in 0.9 M Na_2SO_4, a large part of the attached mass is removed, as shown by a large change in Δf and ΔD. This is interpreted as the covalent grafting competes with the physical adsorption when close to poor solvent conditions are used. This might effectively hamper the chemical grafting process, but to what extent this is the case will depend upon under which flow or stirring condition the grafting is taking place. For the SPR experiments, the gold sensor slides were modified in a container containing the sensor slide and the desired solution under continuous stirring. On the other hand, the QCM sensor chips were modified in the instrument with a continuous flow of 80 µL min^{-1}. Thus, the chemical grafting seems to be less hampered under the flow condition in the QCM experiment than under the stirring conditions used for the preparation of brush layers for the SPR experiments, which is thus giving rise to a higher physical attachment in the latter case.

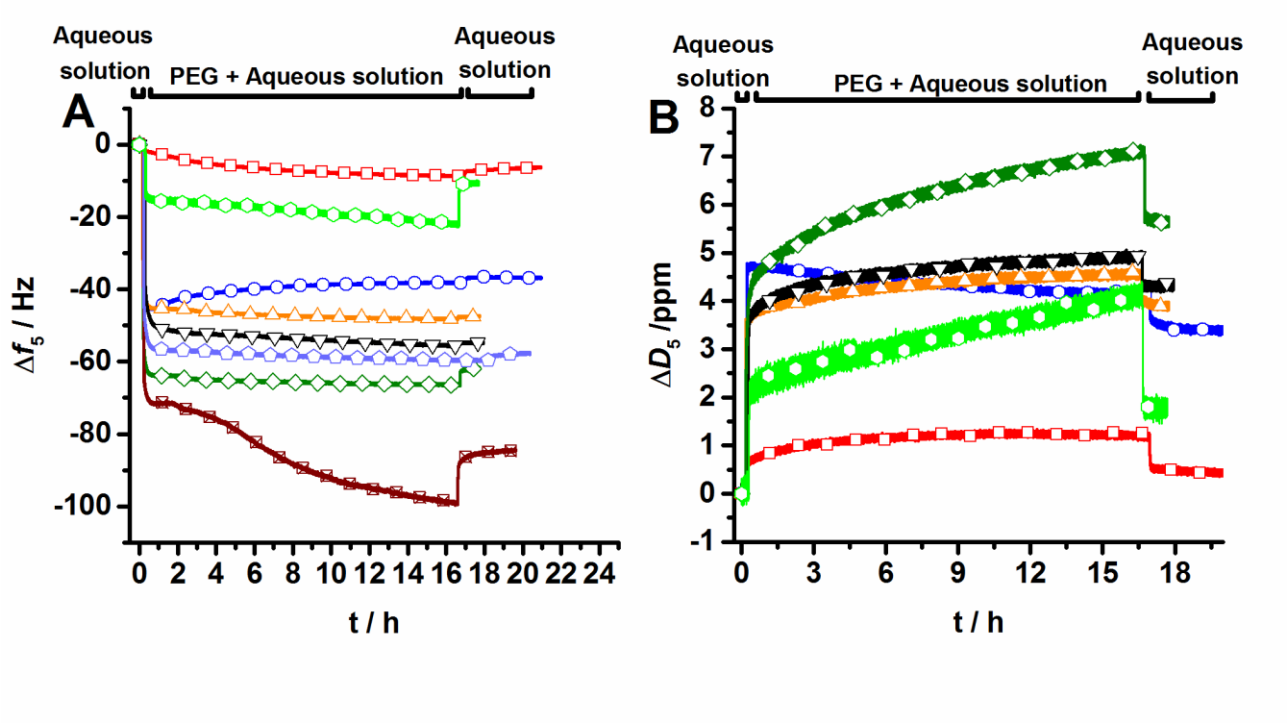

Figure 2. Binding kinetics for (A) Δf_5 and (B) ΔD_5 with time for exposure of 0.6 mg mL^{-1} non-thiolated PEG in water (open squares, red curve) or non-thiolated PEG in 0.9 M Na_2SO_4 (open hexagons, light green) or thiolated PEG in water (open circles, blue curve) or thiolated PEG in Na_2SO_4 being 0.2 (open triangles, orange curve), 0.4 (open inverted triangles, black curve), 0.6 (open pentagon, purple curve), 0.8 (open diamond, green curve) and 0.9 M (crossed squares, dark red curve) Na_2SO_4.

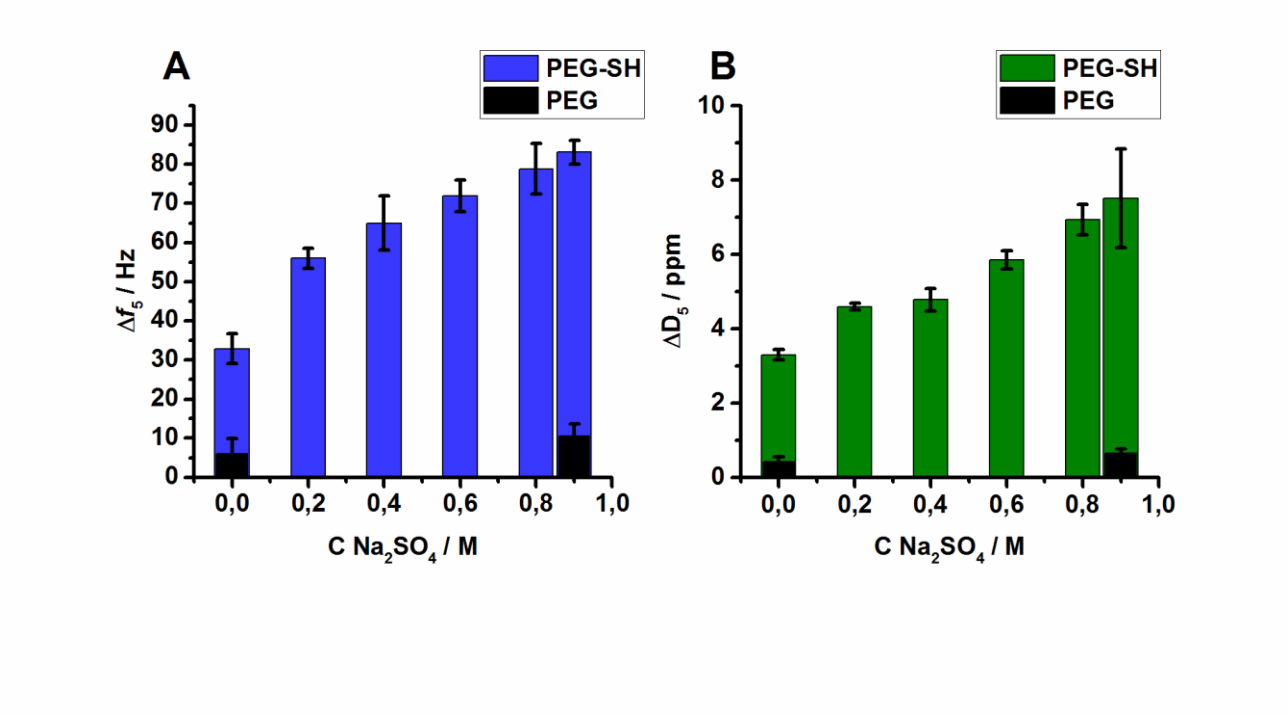

Figure 3. Total changes in (A) Δf_5 and (b) ΔD_5 for 0.6 mg mL^{-1} non-thiolated PEG and thiolated PEG grafted in water or in different concentrations of Na_2SO_4. The values represent the change between a baseline obtained in pure water for the unmodified sensor chips and the modified sensor chips with non-thiolated PEG or thiolated PEG.

Table 1. Values of the Sauerbrey mass, grafting density and brush height obtained from the SPR and QCM-D measurements.

[Na2SO4] (M)	QCM-D Sauerbrey mass (ng cm^{-2})	SPR PEG surface coverage (ng cm^{-2})	SPR PEG Grafting density (Chains nm^{-2})	de Gennes brush height (nm)
0	581±67	216±60	0.26±0.08	11.3±0.9
0.2	990±45	564±65	0.68±0.08	15.6±0.5
0.4	1151±123	863±71	1.04±0.09	18.0±0.4
0.6	1273±72	1328±215	1.60±0.26	20.8±0.9
0.8	1396±115	904±133	1.09±0.16	18.3±0.8
0.9	1470±54	1004±102	1.21±0.12	18.7±0.7

Grafting densities and scaling laws

Since the grafted PEG chains are rather monodisperse and the molecular weight is known, the dry mass obtained from the SPR measurements can be converted to grafting densities. These values, which are presented in Table 1, show that the grafting density varies from 0.26 chains nm^{-2} when the

grafting process is conducted in water, to 1.60 chains nm^{-2} when the grafting process is conducted in 0.6 M Na_2SO_4. The theoretical maximum grafting density for PEG chains is 4.54 chains nm^{-2}, assuming a cross-sectional area of 22 $Å^2$ for PEG chains with a helical conformation.[70] To the best of our knowledge, such high grafting densities have not been reported using the grafting-to technique. By grafting in polymer melts, for which high grafting densities can be obtained due to the minimization of the excluded volume effect, Piehler et al. obtained 0.96 chains nm^{-2} for a PEG 2 kDa.[71] Unsworth and coworkers carried out systematic studies for the PEG grafting of several molecular weights for several deposition times and for different PEG solubility conditions using salts and high temperature. For PEG 2 kDa, a grafting density of 0.98 chains nm^{-2} was obtained after 4 hours and interestingly, saturation of the grafting density was not reached.[24] Using similar grafting techniques for thiolated PEG 5 kDa (as used in this work) a grafting density of 0.12 and 0.24 chains nm^{-2} was obtained for high and low solubility conditions, respectively.[21] Similar values were obtained in a follow up investigation using 4 hours of grafting for the same PEG 5 kDa; 0.12 and 0.3 chains nm^{-2} under high solubility and low solubility conditions, respectively.[22] Other works using PEG 5 kDa reported similar grafting densities as described above. Recently, Emilsson et al. grafted thiolated PEG 5 kDa, obtaining 0.54 chains nm^{-2} under θ-solvent conditions. From the experimental details and plots presented by the authors, we speculate that the grafting process did not exceed 2 hours.[72] Ogaki et al. reported a grafting density of 0.49 chains nm^{-2} using a combination of low solubility and high temperature using PLL-PEG molecules for 20 hours of immobilization.[73] Taylor et al. obtained a grafting density below 0.4 chains nm^{-2} for PEO methyl ether 5 kDa using concentrated homopolymers to reach low solubility conditions with approximately 4 hours of grafting.[20] Efremova et al. obtained 0.21 chains nm^{-2} using PEG 5 kDa conjugated phospholipids at high solubility conditions.[42] Marruecos et al. obtained a grafting density of 0.16 for α-methoxy-ω-triethoxy PEG silane for high solubility conditions and 0.34 chains nm^{-2} for slightly lower solubility conditions.[44]

These values obtained in the literature illustrate that, for good solvent conditions grafting densities between 0.1 - 0.2 chains nm^{-2} and for low solubility conditions, grafting densities between 0.3 - 0.6 chains nm^{-2} are obtained for PEG 5 kDa using the grafting-to approach with diluted polymer solutions. In all cases, except grafting the PLL-PEG copolymer,[73] deposition times below 4 hours were used, and the comparison of these values with the ones obtained in this work highlights the importance of immobilization time in order to obtain high grafting densities. In our case, all the prepared PEG layers were deposited for at least 16 h either grafted with stirring in a container or with a continuous flow in a QCM-D cell. The importance of the time for immobilization in conditions

where the excluded volume interactions plays a role has been discussed previously by Penn and coworkers.[50, 54, 57] In addition to our work, similar high grafting densities (1.27 chains nm^{-2}) have been reported previously by Arcot et al. using mixtures of organic solvents to obtain low solubility conditions for PEG 5 kDa.[25] Using PEG melts at high temperatures also similar grafting densities were obtained, Zdyrko et al. obtained 1.2 chains nm^{-2} at saturation conditions for a PEG 5 kDa.[74] Regardless of the methods used to calculate the grafting density and the differences between the studies, to best of our knowledge, these are the highest grafting densities obtained for a PEG 5 kDa grafted using the grafting-to method.

As the limiting factor for a high grafting density using a grafting-to approach is the steric hindrance, the coil size of the unperturbed polymer is believed to be a decisive parameter. The coil size can de described by the Flory radius:

$$R_F = b\left(\frac{aN}{b}\right)^{\upsilon}$$

where a is the monomer size (a = 0.28 nm for PEG in water),[75-76] b is the Kuhn length (b = 0.73 nm is used here as an intermediate value of data obtained in the literature)[75, 77-78] and N is the number of monomers in the chain (113 for PEG 5 kDa). The exponent υ has a magnitude which depends on the solvent quality and will vary from 3/5 in good solvent conditions to 1/2 in θ-solvent conditions. Using this relationship, when the polymer is changing from good solvent condition (pure water) toward θ-solvent condition (high salt), the Flory radius will vary from 7.0 nm to 4.8 nm which indicates that there is a strong correlation between the coil size and the grafting density. The higher grafting densities obtained during binding in the presence of Na_2SO_4 will result in a significant chain extension when the grafted layers are exposed to good solvent conditions, as illustrated in Fig. 4. The values can be estimated by the Alexander de Gennes scaling relation:[7, 79]

$$H = \left(\frac{\sigma}{3}\right)^{1/3} b^{2/3} aN$$

where σ is the grafting density. Using this approximation, the brush heights in the good solvent condition are found to vary from approximately 11 nm for the lowest grafting density to approximately 20 nm for the highest grafting density (Table 1). This indicates that the PEG layer grafted in water (the good solvent) has a thickness which is slightly less than two times the Flory radius, which is interpreted as a layer consisting of closed packed coils; that is, a film consisting of PEG in a mushroom conformation. However, for the PEG layer grafted at θ-solvent conditions, the

layer extends to a thickness which corresponds to approximately two thirds of the total contour length of the PEG chains, $L = aN$ = 32 nm, and approximately 3 times the Flory radius, and is thus obtaining a brush conformation.

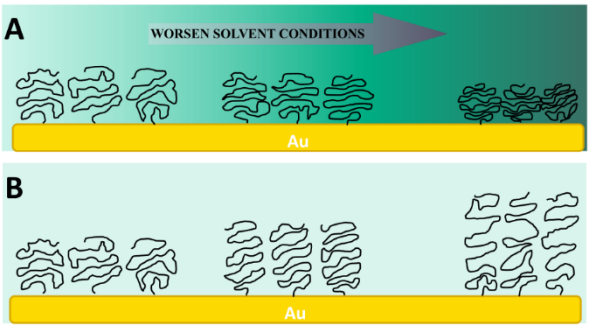

Figure 4. (A) Diagram showing the PEG grafting process onto a gold surface for different solubility conditions and (B) the expansion of the polymers when solubility conditions are changed for the grafted polymer.

The effect of Na_2SO_4 on the grafting kinetics

A closer look at Fig. 2 shows that the grafting process also changes in a more qualitative manner depending on the concentration of Na_2SO_4. By plotting Δf against ΔD, time is explicitly removed from the data. In the following we use such plots for a better interpretation of the changes in polymer conformation as the layer builds up. These plots typically show sections with different gradients. The gradient normalizes the energy dissipation of the adlayer to mass, so changes in the slope indicate changes in the adsorbate-surface interactions or conformational changes during the adsorption process.[80-82]

Fig. 5 shows the curves corresponding to adsorption of non-thiolated PEG and grafting of thiolated PEG under different solubility conditions (for clarity, the washing step has been omitted in this discussion). In this figure the density of symbols is correlated with the time, meaning that a region with higher density of symbols corresponds to slower kinetics than a section with lower density of symbols. The adsorption of non-thiolated PEG onto the gold surface is characterized by a linear response of Δf vs ΔD (Fig. 5(A), red curve). The low adsorbed amount (considering the small value of $\Delta f_5 \sim 1$ Hz) and the stiff film formed (small $\Delta D_5 \sim 1 \times 10^{-6}$) on the surface, indicate that a few PEG chains are adsorbed in a rather flat conformation. Nevertheless, the interaction is weak and after the

washing step, most of the adsorbed polymers are released from the surface, as previously discussed in relation to Fig. 2 (red curve).

For thiolated PEG grafted in pure water (Fig. 5(A), blue curve), three different sections are observed on the curve; the arrows in the figure show the direction of the grafting with time: (I) a rapid increase of -Δ*f* and Δ*D*, (II) a section characterized by a moderate change in -Δ*f* but not of Δ*D*, and (III) a continuous decrease in -Δ*f* but no substantial change in Δ*D*. The three sections are interpreted as: (I) a rapid initial grafting to a bare surface due to the high affinity of the thiol group to the surface controlled by diffusion of the polymer to the surface, (II) a slower grafting for which surface saturation is reached, and (III) reorganization of grafted PEG due to thiol-gold mobility on the gold surface.[83-84] Note that Δ*D* does not vary substantially in (II) and (III), indicating that the flexibility of the films is barely altered. Similar binding profiles have been reported previously for thiolated polymers even if the kinetics of formation have not been discussed.[85-87] Here, this behavior is interpreted as a lack of a transition from a mushroom conformation to a brush conformation.

In the presence of salt, the grafting process shows a different behavior. In Fig. 5(B), the sections are marked for 0.8 M Na_2SO_4 (green curve) but are observed for all other conditions: (I) rapid increase of -Δ*f* and Δ*D*, (II) increase in the slope due to a substantial increase in Δ*D* and (III) a new change in the slope characterized by a slow-down of the increase of -Δ*f* in relation to Δ*D*. For the analysis of the different grafting processes in the presence of salt, it should be taken into consideration that the size of the polymer decreases with increased concentration of Na_2SO_4. For the highest salt concentrations, the aqueous salt solutions are close to θ-solvent conditions with respect to PEG, and the Flory radius will be reduced to approximately 4.8 nm. The reduced size of the coil creates a smaller excluded volume effect when grafted, allowing a greater number of coils to access the surface and be grafted. The data for grafting in the 0.9 M Na_2SO_4 solution was disregarded in this discussion due to the possible physical adsorption discussed previously. The changes of the features of the plot in Fig. 5(B) are interpreted as (I) a rapid initial grafting to a bare surface due to the high surface affinity of the thiol group, which is controlled by diffusion of the polymer that continues until saturation is reached and a monolayer of PEG coils is formed, (II) reorganization of the layer due to the mobility of the gold-sulfur bond, which is creating a slightly more viscoelastic film and (III) an extension of the PEG chains from a mushroom conformation to a more extended brush conformation.

Due to dehydration of polymer chains, it is predicted that the polymer layers will become more rigid with increasing Na_2SO_4 concentration, which is observed as a decrease in the initial values of Δ*D*

during grafting in the section I in Fig. 5(B). The process in section I in the presence of salt show the same behavior as in the absence of salt and are interpreted as a Brownian diffusion of the polymers to the surface. In sections II and III, the dissipation increases rapidly with a small increase of -Δ*f* which is an indication of a polymer conformational change to a more extended conformation. We interpret the two different sections as a result of a reorganization of the mobile gold-sulfur bonds which is subsequently followed by stretching of the polymer chains.

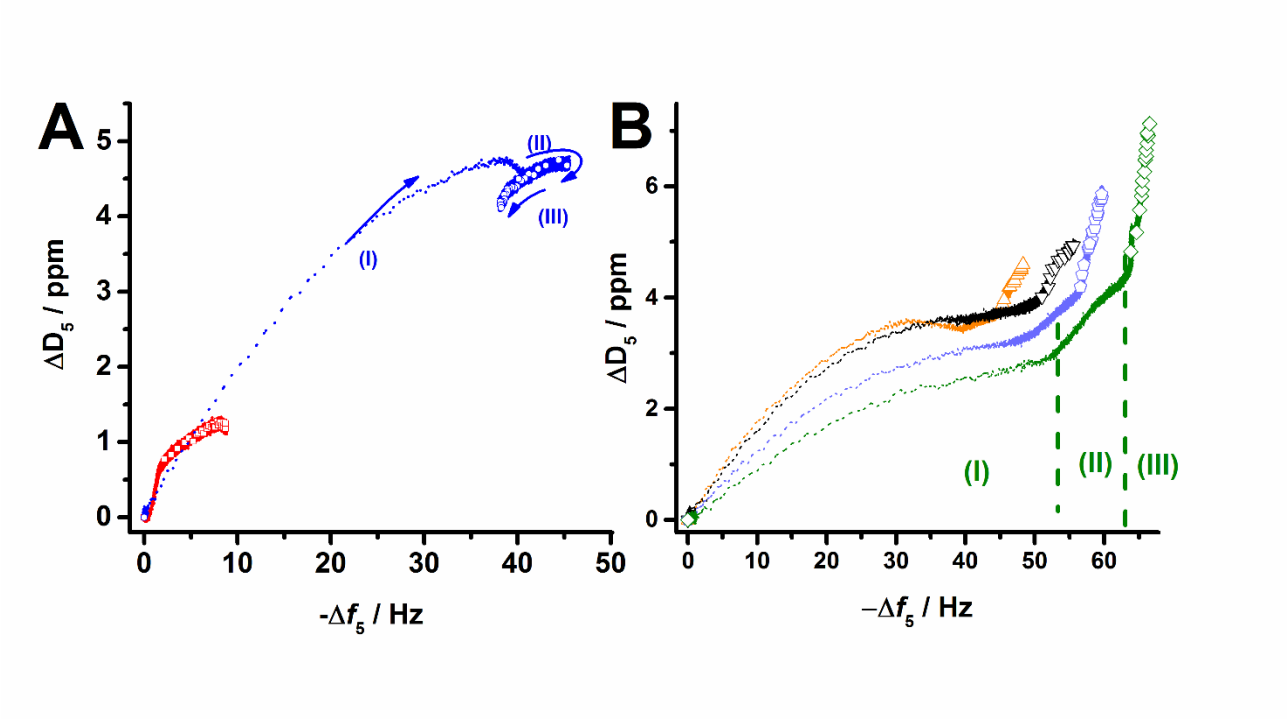

Figure 5. Plot of Δf_5 vs ΔD_5 for the grafting process of PEG in the absence (A) and presence of Na_2SO_4 (B). Curves represent: PEG in water (red), thiolated PEG in water (dark blue), thiolated PEG in 0.2 M (orange), 0.4 M (black), 0.6 M (light blue) and 0.8 M (dark green) Na_2SO_4. The roman numerals indicate changes in the slope of the curves.

Resistance to bovine serum albumin adsorption

In the scope of the high grafting densities obtained, protein resistance was evaluated for usage as a benchmark in fouling studies.[35, 88-90] Concentration and pH relevant to physiological conditions were used due to the interest in developing surfaces that resist bioadhesion. Relevant protein concentrations for bovine serum albumin (BSA) for physiological conditions (0.01 to 5 mg mL^{-1}) and PBS pH 7.40 in 137 mM KCl were used.[91]

Low (0.01 and 0.1 mg mL^{-1}) and high (1 and 5 mg mL^{-1}) BSA concentrations were flowed over surfaces with a PEG layer grafted in water, a PEG layer grafted in 0.9 M Na_2SO_4 and a non-modified QCM-D gold sensor chips. Between each BSA injection, buffer was injected to remove weakly adsorbed BSA from the surface. Fig. 6 shows the change in frequency for BSA injections for non-modified gold chips (black line) and modified gold chips using PEG in water (green line) or PEG in 0.9 M Na_2SO_4 (red line). No detectable BSA adsorption was observed for the surfaces modified with PEG grafted in 0.9 M Na_2SO_4.

The adsorbed amount of BSA was determined using the Sauerbrey equation for Δf_3 before and after BSA adsorption in buffer solution (Table 2). In doing so, the values of the mass reported in Table 2 are underestimated due to viscoelastic contributions and the values represent the wet mass. In the non-modified gold sensor chips, high amounts of BSA were adsorbed even for the lowest BSA concentration injected (92.1 ng cm^{-2}). On the other hand, the polymer modified surfaces showed low fouling (3.9 ng cm^{-2}) and Δf_3 changes below the detection limit of the instrument for the gold chips modified with PEG grafted in water and 0.9 Na_2SO_4, respectively. For the gold chips modified with PEG grafted in Na_2SO_4, no measurable BSA adsorption was observed even for the highest concentration of BSA (5 mg mL^{-1}).

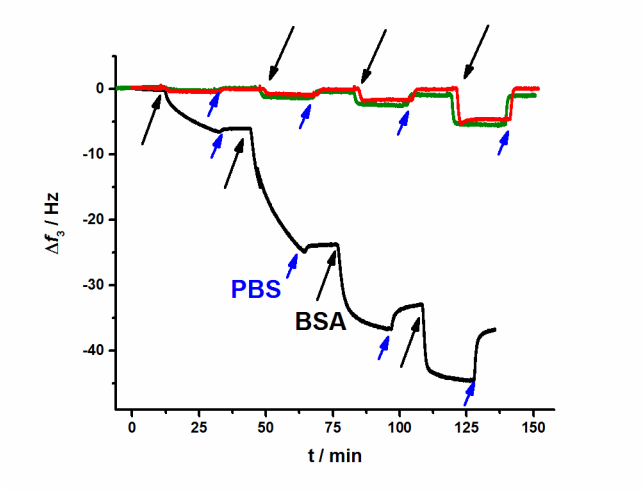

Figure 6. QCM-D data showing the adsorption of BSA on surfaces using 0.01, 0.1, 1 and 5 mg mL^{-1} BSA solutions on a PEG layer grafted in water (green), on an PEG layer grafted in 0.9 M Na_2SO_4 (red) and an non-modified gold surface (black). Black arrows indicate BSA injection and blue arrows indicate injection of PBS. Experimental conditions: 80 µL mL^{-1}, 100 mM PBS pH 7.4.

Table 2. QCM-D Sauerbrey mass calculated for the 3th overtone of the amount of BSA adsorbed onto gold non-modified surfaces and PEG grafted either in water or Na_2SO_4. Experimental conditions: 80 µL mL^{-1}, 100 mM PBS pH 7.4.

Surface modification	Sauerbrey mass BSA 0.01% (ng cm^{-2})	Sauerbrey mass BSA 0.1% (ng cm^{-2})	Sauerbrey mass BSA 1% (ng cm^{-2})	Sauerbrey mass BSA 5% (ng cm^{-2})
Non-modified gold sensor chip	92.1±11.2	399.7±19.4	563.1±4.1	621.1±7.7
PEG (pure water)	3.9±2.7	12.6±1.0	17.9±2.5	20.1±1.1
PEG (0.9 M Na_2SO_4)	Below detection limit	Below detection limit	Below detection limit	Below detection limit

CONCLUSIONS

Fabrication of PEG brush layers with a variation in grafting densities was obtained by altering the concentration of Na_2SO_4 in aqueous solutions during the grafting process. Na_2SO_4 is known to have a strong salting-out effect, and its presence changed the solubility properties of water towards PEG. The quantitative values of the grafting densities obtained from the SPR measurements were employed to calculate the Alexander de Gennes brush layer thicknesses and the result of this, indicates a mushroom conformation for a PEG layer grafted in water and a more extended brush conformation for PEG layers grafted in the presence of Na_2SO_4. The conclusions are further supported by the QCM-D measurement where higher values of Δf and ΔD are observed for PEG layers grafted with salt than without salt.

The grafting process of thiolated PEG layers was further studied in situ by QCM-D, which in the absence of salt showed a previously not described grafting kinetics. The data for thiolated PEG grafted in the presence of salt experiences a transition from a mushroom to a more extended conformation. The transition needs a certain immobilization time to occur, which is different for each salt concentration. The highest dissipation change values at the end of the conformational change were found for the highest Na_2SO_4 concentrations used. Using the method described in this work grafting densities up to 1.60 chains nm^{-2} were obtained, which to the best of our knowledge is among the highest grafting densities reported for PEG 5 kDa.

Finally, the prepared PEG surfaces showed significantly higher resistance to BSA adsorption than unmodified gold and for the PEG layer with the highest grafting density, no detectable adsorption was observed.

ACKNOWLEDGMENTS

The authors acknowledge the financial support of the Maritime Foundation and the Danish Council for Independent Research (Project ID: Multi-function anti-fouling bio-active surfaces; DFF – 5054-00196). We gratefully acknowledge Dr. N. Grandqvist for useful discussions regarding the fitting and modeling of SPR.

ASSOCIATED CONTENT

Supporting Information: Image showing thiolated PEG dissolved in increasing concentrations of Na_2SO_4 to assess the cloud point conditions and plot of Δf for the grafting process of PEG in the presence of 0.8 M Na_2SO_4 and stability of the grafted layer in H_2O and Na_2SO_4. This material is available free of charge via the Internet at http://pubs.acs.org.

REFERENCES

1. Zhao, B.; Brittain, W. J., Polymer brushes: surface-immobilized macromolecules. *Prog. Polym. Sci.* **2000,** *25* (5), 677-710.
2. Fristrup, C. J.; Jankova, K.; Hvilsted, S., Surface-initiated atom transfer radical polymerization-a technique to develop biofunctional coatings. *Soft Matter* **2009,** *5* (23), 4623-4634.
3. Kato, K.; Uchida, E.; Kang, E.-T.; Uyama, Y.; Ikada, Y., Polymer surface with graft chains. *Prog. Polym. Sci.* **2003,** *28* (2), 209-259.
4. Currie, E. P. K.; Norde, W.; Cohen Stuart, M. A., Tethered polymer chains: surface chemistry and their impact on colloidal and surface properties. *Adv. Colloid Interfac.* **2003,** *100*, 205-265.
5. Bhat, R. R.; Tomlinson, M. R.; Wu, T.; Genzer, J., Surface-Grafted Polymer Gradients: Formation, Characterization, and Applications. In *Surface-Initiated Polymerization II*, Jordan, R., Ed. Springer Berlin Heidelberg: Berlin, Heidelberg, 2006; pp 51-124.
6. Stuart, M. A. C.; Huck, W. T. S.; Genzer, J.; Muller, M.; Ober, C.; Stamm, M.; Sukhorukov, G. B.; Szleifer, I.; Tsukruk, V. V.; Urban, M.; Winnik, F.; Zauscher, S.; Luzinov, I.; Minko, S., Emerging applications of stimuli-responsive polymer materials. *Nat. Mater.* **2010,** *9* (2), 101-113.
7. de Gennes, P. G., Conformations of Polymers Attached to an Interface. *Macromolecules* **1980,** *13* (5), 1069-1075.
8. Senaratne, W.; Andruzzi, L.; Ober, C. K., Self-Assembled Monolayers and Polymer Brushes in Biotechnology: Current Applications and Future Perspectives. *Biomacromolecules* **2005,** *6* (5), 2427-2448.
9. Milner, S. T., Polymer Brushes. *Science* **1991,** *251* (4996), 905-914.
10. Matyjaszewski, K.; Miller, P. J.; Shukla, N.; Immaraporn, B.; Gelman, A.; Luokala, B. B.; Siclovan, T. M.; Kickelbick, G.; Vallant, T.; Hoffmann, H.; Pakula, T., Polymers at Interfaces: Using Atom Transfer Radical Polymerization in the Controlled Growth of Homopolymers and Block Copolymers from Silicon Surfaces in the Absence of Untethered Sacrificial Initiator. *Macromolecules* **1999,** *32* (26), 8716-8724.
11. Baum, M.; Brittain, W. J., Synthesis of Polymer Brushes on Silicate Substrates via Reversible Addition Fragmentation Chain Transfer Technique. *Macromolecules* **2002,** *35* (3), 610-615.
12. Matyjaszewski, K., Atom Transfer Radical Polymerization (ATRP): Current Status and Future Perspectives. *Macromolecules* **2012,** *45* (10), 4015-4039.
13. Hawker, C. J.; Bosman, A. W.; Harth, E., New Polymer Synthesis by Nitroxide Mediated Living Radical Polymerizations. *Chem. Rev.* **2001,** *101* (12), 3661-3688.
14. Kingshott, P.; Thissen, H.; Griesser, H. J., Effects of cloud-point grafting, chain length, and density of PEG layers on competitive adsorption of ocular proteins. *Biomaterials* **2002,** *23* (9), 2043-2056.
15. Emoto, K.; Harris, J. M.; Van Alstine, J. M., Grafting Poly(ethylene glycol) Epoxide to Amino-Derivatized Quartz: Effect of Temperature and pH on Grafting Density. *Anal. Chem.* **1996,** *68* (21), 3751-3757.
16. Zdyrko, B.; Luzinov, I., Polymer Brushes by the "Grafting to" Method. *Macromol. Rapid Comm.* **2011,** *32* (12), 859-869.
17. Minko, S.; Patil, S.; Datsyuk, V.; Simon, F.; Eichhorn, K.-J.; Motornov, M.; Usov, D.; Tokarev, I.; Stamm, M., Synthesis of Adaptive Polymer Brushes via "Grafting To" Approach from Melt. *Langmuir* **2002,** *18* (1), 289-296.
18. Sofia, S. J.; Premnath, V.; Merrill, E. W., Poly(ethylene oxide) Grafted to Silicon Surfaces: Grafting Density and Protein Adsorption. *Macromolecules* **1998,** *31* (15), 5059-5070.
19. Huang, H.; Penn, L. S., Dense Tethered Layers by the "Grafting-To" Approach. *Macromolecules* **2005,** *38* (11), 4837-4843.
20. Taylor, W.; Jones, R. A. L., Producing High-Density High-Molecular-Weight Polymer Brushes by a "Grafting to" Method from a Concentrated Homopolymer Solution. *Langmuir* **2010,** *26* (17), 13954-13958.
21. Unsworth, L. D.; Sheardown, H.; Brash, J. L., Polyethylene oxide surfaces of variable chain density by chemisorption of PEO-thiol on gold: Adsorption of proteins from plasma studied by radiolabelling and immunoblotting. *Biomaterials* **2005,** *26* (30), 5927-5933.

22. Unsworth, L. D.; Tun, Z.; Sheardown, H.; Brash, J. L., Chemisorption of thiolated poly(ethylene oxide) to gold: surface chain densities measured by ellipsometry and neutron reflectometry. *J. Colloid Interf. Sci.* **2005,** *281* (1), 112-121.
23. Tun, Z.; Unsworth, L. D.; Brash, J. L.; Sheardown, H., Determination of graft density of substrate-supported polymer films. *Physica B* **2006,** *385–386, Part 1* (0), 697-699.
24. Unsworth, L. D.; Sheardown, H.; Brash, J. L., Protein-Resistant Poly(ethylene oxide)-Grafted Surfaces: Chain Density-Dependent Multiple Mechanisms of Action. *Langmuir* **2008,** *24* (5), 1924-1929.
25. Arcot, L.; Ogaki, R.; Zhang, S.; Meyer, R. L.; Kingshott, P., Optimizing the surface density of polyethylene glycol chains by grafting from binary solvent mixtures. *Appl. Surf. Sci.* **2015,** *341*, 134-141.
26. Jeon, S. I.; Lee, J. H.; Andrade, J. D.; De Gennes, P. G., Protein—surface interactions in the presence of polyethylene oxide: I. Simplified theory. *J. Colloid Interf. Sci.* **1991,** *142* (1), 149-158.
27. Banerjee, I.; Pangule, R. C.; Kane, R. S., Antifouling Coatings: Recent Developments in the Design of Surfaces That Prevent Fouling by Proteins, Bacteria, and Marine Organisms. *Adv. Mat.* **2011,** *23* (6), 690-718.
28. Hoffman, A. S., Hydrogels for biomedical applications. *Adv. Drug Delivery Reviews* **2002,** *54* (1), 3-12.
29. Zhao, C.; Li, L.-Y.; Guo, M.-M.; Zheng, J., Functional polymer thin films designed for antifouling materials and biosensors. *Chemical Papers* **2012,** *66* (5), 323-339.
30. Gifford, R.; Kehoe, J. J.; Barnes, S. L.; Kornilayev, B. A.; Alterman, M. A.; Wilson, G. S., Protein interactions with subcutaneously implanted biosensors. *Biomaterials* **2006,** *27* (12), 2587-2598.
31. Campoccia, D.; Montanaro, L.; Arciola, C. R., A review of the biomaterials technologies for infection-resistant surfaces. *Biomaterials* **2013,** *34* (34), 8533-8554.
32. Dobretsov, S.; Abed, R. M. M.; Teplitski, M., Mini-review: Inhibition of biofouling by marine microorganisms. *Biofouling: The Journal of Bioadhesion and Biofilm Research* **2013,** *29* (4), 423-441.
33. Gittens, J. E.; Smith, T. J.; Suleiman, R.; Akid, R., Current and emerging environmentally-friendly systems for fouling control in the marine environment. *Biotechnol. Adv.* **2013,** *31* (8), 1738-1753.
34. Kochkodan, V.; Hilal, N., A comprehensive review on surface modified polymer membranes for biofouling mitigation. *Desalination* **2015**, 356 (Supplement C), 187-207.
35. Norde, W.; Gage, D., Interaction of Bovine Serum Albumin and Human Blood Plasma with PEO-Tethered Surfaces: Influence of PEO Chain Length, Grafting Density, and Temperature. *Langmuir* **2004,** *20* (10), 4162-4167.
36. Unsworth, L. D.; Sheardown, H.; Brash, J. L., Protein Resistance of Surfaces Prepared by Sorption of End-Thiolated Poly(ethylene glycol) to Gold: Effect of Surface Chain Density. *Langmuir* **2005,** *21* (3), 1036-1041.
37. Zheng, J.; Li, L.; Chen, S.; Jiang, S., Molecular Simulation Study of Water Interactions with Oligo (Ethylene Glycol)-Terminated Alkanethiol Self-Assembled Monolayers. *Langmuir* **2004,** *20* (20), 8931-8938.
38. Zolk, M.; Eisert, F.; Pipper, J.; Herrwerth, S.; Eck, W.; Buck, M.; Grunze, M., Solvation of Oligo(ethylene glycol)-Terminated Self-Assembled Monolayers Studied by Vibrational Sum Frequency Spectroscopy. *Langmuir* **2000,** *16* (14), 5849-5852.
39. Sant, S.; Poulin, S.; Hildgen, P., Effect of polymer architecture on surface properties, plasma protein adsorption, and cellular interactions of pegylated nanoparticles. *J.Biomed. Mat. Res. A* **2008,** *87A* (4), 885-895.
40. Leckband, D.; Sheth, S.; Halperin, A., Grafted poly(ethylene oxide) brushes as nonfouling surface coatings. *J. Biomater. Sci. Polym.* **1999,** *10* (10), 1125-47.
41. Bloustine, J.; Virmani, T.; Thurston, G. M.; Fraden, S., Light Scattering and Phase Behavior of Lysozyme-Poly(Ethylene Glycol) Mixtures. *Phys. Rev. Lett.* **2006,** *96* (8), 087803.
42. Efremova, N. V.; Sheth, S. R.; Leckband, D. E., Protein-Induced Changes in Poly(ethylene glycol) Brushes: Molecular Weight and Temperature Dependence. *Langmuir* **2001,** *17* (24), 7628-7636.
43. Sheth, S. R.; Leckband, D., Measurements of attractive forces between proteins and end-grafted poly(ethylene glycol) chains. *PNAS* **1997,** *94* (16), 8399-8404.

44. Faulón Marruecos, D.; Kastantin, M.; Schwartz, D. K.; Kaar, J. L., Dense Poly(ethylene glycol) Brushes Reduce Adsorption and Stabilize the Unfolded Conformation of Fibronectin. *Biomacromolecules* **2016,** *17* (3), 1017-1025.
45. Jin, J.; Han, Y.; Zhang, C.; Liu, J.; Jiang, W.; Yin, J.; Liang, H., Effect of grafted PEG chain conformation on albumin and lysozyme adsorption: A combined study using QCM-D and DPI. *Colloid Surface B* **2015,** *136*, 838-844.
46. Evans, J. W., Random and cooperative sequential adsorption. *Rev. Mod. Phys.* **1993,** *65* (4), 1281-1329.
47. Talbot, J.; Tarjus, G.; Van Tassel, P. R.; Viot, P., From car parking to protein adsorption: an overview of sequential adsorption processes. *Colloid Surface A* **2000,** *165* (1), 287-324.
48. Hinrichsen, E. L.; Feder, J.; Jøssang, T., Geometry of random sequential adsorption. *J. Stat. Phys.* **1986,** *44* (5), 793-827.
49. Ligoure, C.; Leibler, L., Thermodynamics and kinetics of grafting end-functionalized polymers to an interface. *J. Phys. France* **1990,** *51* (12), 1313-1328.
50. Sha, X.; Xu, X.; Sohlberg, K.; Loll, P. J.; Penn, L. S., Evidence that three-regime kinetics is inherent to formation of a polymer brush by a grafting-to approach. *RSC Adv.* **2014,** *4* (79), 42122-42128.
51. Lee, H.-S.; Penn, L. S., Evidence for Relative Radius of Gyration as the Criterion for Selective Diffusion Behavior of Polymer Brushes. *Langmuir* **2009,** *25* (14), 7983-7989.
52. Huang, H.; Cammers, A.; Penn, L. S., Grafting of Free Chains in the Presence of Preexisting Polymer Brushes. *Macromolecules* **2006,** *39* (20), 7064-7070.
53. Huang, H.; Penn, L. S.; Quirk, R. P.; Cheong, T. H., Effect of Segmental Adsorption on the Tethering of End-Functionalized Polymer Chains. *Macromolecules* **2004,** *37* (2), 516-523.
54. Huang, H.; Rankin, S. E.; Penn, L. S.; Quirk, R. P.; Cheong, T. H., Transition from Mushroom to Brush during Formation of a Tethered Layer. *Langmuir* **2004,** *20* (14), 5770-5775.
55. Huang, H.; Penn, L. S.; Quirk, R. P.; Cheong, T. H., Kinetics of Sequential Tethering in Formation of Mixed Layers. *Macromolecules* **2004,** *37* (15), 5807-5813.
56. Penn, L. S.; Hunter, T. F.; Quirk, R. P.; Lee, Y., Deactivation of Epoxide-Derivatized Surfaces. *Macromolecules* **2002,** *35* (7), 2859-2860.
57. Penn, L. S.; Huang, H.; Sindkhedkar, M. D.; Rankin, S. E.; Chittenden, K.; Quirk, R. P.; Mathers, R. T.; Lee, Y., Formation of Tethered Nanolayers: Three Regimes of Kinetics. *Macromolecules* **2002,** *35* (18), 7054-7066.
58. Penn, L. S.; Hunter, T. F.; Lee, Y.; Quirk, R. P., Grafting Rates of Amine-Functionalized Polystyrenes onto Epoxidized Silica Surfaces. *Macromolecules* **2000,** *33* (4), 1105-1107.
59. Winspall 3.1 it is freely available software developed by the Max-Planck Institute for Polymer Research (Mainz, G. a. f. R. T. G., Framersheim, Germany; http://www.res-tec.de/downloads.html, accessed 03.03.2017.
60. Granqvist, N.; Liang, H.; Laurila, T.; Sadowski, J.; Yliperttula, M.; Viitala, T., Characterizing Ultrathin and Thick Organic Layers by Surface Plasmon Resonance Three-Wavelength and Waveguide Mode Analysis. *Langmuir* **2013,** *29* (27), 8561-8571.
61. Daniel R. Bloch; Akihiro Abe; E. A. Grulke; Edmund H. Immergut; Brandrup, J., *Polymer Handbook*. 4th Edition ed.; John Wiley & Sons Inc: 2003.
62. Reviakine, I.; Johannsmann, D.; Richter, R. P., Hearing What You Cannot See and Visualizing What You Hear: Interpreting Quartz Crystal Microbalance Data from Solvated Interfaces. *Anal. Chem.* **2011,** *83* (23), 8838-8848.
63. Thormann, E., On understanding of the Hofmeister effect: how addition of salt alters the stability of temperature responsive polymers in aqueous solutions. *RSC Adv.* **2012,** *2* (22), 8297-8305.
64. Cacace, M. G.; Landau, E. M.; Ramsden, J. J., The Hofmeister series: salt and solvent effects on interfacial phenomena. *Quartely reviews of biophysics* **1997,** *30* (3), 241-77.

65. Liang, H.; Miranto, H.; Granqvist, N.; Sadowski, J. W.; Viitala, T.; Wang, B.; Yliperttula, M., Surface plasmon resonance instrument as a refractometer for liquids and ultrathin films. *Sensor Actuat. B-Chem.* **2010,** *149* (1), 212-220.
66. Peterlinz, K. A.; Georgiadis, R., Two-color approach for determination of thickness and dielectric constant of thin films using surface plasmon resonance spectroscopy. *Opt. Comm.* **1996,** *130* (4), 260-266.
67. Heuberger, M.; Drobek, T.; Vörös, J., About the Role of Water in Surface-Grafted Poly(ethylene glycol) Layers. *Langmuir* **2004,** *20* (22), 9445-9448.
68. Iruthayaraj, J.; Olanya, G.; Claesson, P. M., Viscoelastic Properties of Adsorbed Bottle-brush Polymer Layers Studied by Quartz Crystal Microbalance — Dissipation Measurements. *J. Phys. Chem. C* **2008,** *112* (38), 15028-15036.
69. Macakova, L.; Blomberg, E.; Claesson, P. M., Effect of Adsorbed Layer Surface Roughness on the QCM-D Response: Focus on Trapped Water. *Langmuir* **2007,** *23* (24), 12436-12444.
70. Harder, P.; Grunze, M.; Dahint, R.; Whitesides, G. M.; Laibinis, P. E., Molecular Conformation in Oligo(ethylene glycol)-Terminated Self-Assembled Monolayers on Gold and Silver Surfaces Determines Their Ability To Resist Protein Adsorption. *J. Phys. Chem. B* **1998,** *102* (2), 426-436.
71. Piehler, J.; Brecht, A.; Valiokas, R.; Liedberg, B.; Gauglitz, G., A high-density poly(ethylene glycol) polymer brush for immobilization on glass-type surfaces. *Biosens. Bioelectron.* **2000,** *15* (9–10), 473-481.
72. Emilsson, G.; Schoch, R. L.; Feuz, L.; Höök, F.; Lim, R. Y. H.; Dahlin, A. B., Strongly Stretched Protein Resistant Poly(ethylene glycol) Brushes Prepared by Grafting-To. *ACS Appl. Mat. Inter.* **2015,** *7* (14), 7505-7515.
73. Ogaki, R.; Zoffmann Andersen, O.; Jensen, G. V.; Kolind, K.; Kraft, D. C. E.; Pedersen, J. S.; Foss, M., Temperature-Induced Ultradense PEG Polyelectrolyte Surface Grafting Provides Effective Long-Term Bioresistance against Mammalian Cells, Serum, and Whole Blood. *Biomacromolecules* **2012,** *13* (11), 3668-3677.
74. Zdyrko, B.; Varshney, S. K.; Luzinov, I., Effect of Molecular Weight on Synthesis and Surface Morphology of High-Density Poly(ethylene glycol) Grafted Layers. *Langmuir* **2004,** *20* (16), 6727-6735.
75. Oesterhelt, F.; Rief, M.; Gaub, H. E., Single molecule force spectroscopy by AFM indicates helical structure of poly(ethylene-glycol) in water. *New J. Phys.* **1999,** *1* (1), 6.
76. Mark, J. E.; Flory, P. J., The Configuration of the Polyoxyethylene Chain. *J. Am. Chem. Soc.* **1965,** *87* (7), 1415-1423.
77. Kienberger, F.; Pastushenko, V. P.; Kada, G.; Gruber, H. J.; Riener, C.; Schindler, H.; Hinterdorfer, P., Static and Dynamical Properties of Single Poly(Ethylene Glycol) Molecules Investigated by Force Spectroscopy. *Single Molecules* **2000,** *1* (2), 123-128.
78. Lee, H.; Venable, R. M.; MacKerell, A. D.; Pastor, R. W., Molecular Dynamics Studies of Polyethylene Oxide and Polyethylene Glycol: Hydrodynamic Radius and Shape Anisotropy. *Biophys. J.* **2008,** *95* (4), 1590-1599.
79. De Gennes, P. G., Scaling theory of polymer adsorption. *J. Phys. France* **1976,** *37* (12), 1445-1452.
80. Sedeva, I. G.; Fetzer, R.; Fornasiero, D.; Ralston, J.; Beattie, D. A., Adsorption of modified dextrins to a hydrophobic surface: QCM-D studies, AFM imaging, and dynamic contact angle measurements. *J. Colloid Interf. Sci.* **2010,** *345* (2), 417-426.
81. Monkawa, A.; Ikoma, T.; Yunoki, S.; Yoshioka, T.; Tanaka, J.; Chakarov, D.; Kasemo, B., Fabrication of hydroxyapatite ultra-thin layer on gold surface and its application for quartz crystal microbalance technique. *Biomaterials* **2006,** *27* (33), 5748-5754.
82. Höök, F.; Rodahl, M.; Brzezinski, P.; Kasemo, B., Energy Dissipation Kinetics for Protein and Antibody−Antigen Adsorption under Shear Oscillation on a Quartz Crystal Microbalance. *Langmuir* **1998,** *14* (4), 729-734.

83. Bürgi, T., Properties of the gold-sulphur interface: from self-assembled monolayers to clusters. *Nanoscale* **2015,** *7* (38), 15553-15567.
84. McCarley, R. L.; Dunaway, D. J.; Willicut, R. J., Mobility of the alkanethiol-gold (111) interface studied by scanning probe microscopy. *Langmuir* **1993,** *9* (11), 2775-2777.
85. Slavin, S.; Soeriyadi, A. H.; Voorhaar, L.; Whittaker, M. R.; Becer, C. R.; Boyer, C.; Davis, T. P.; Haddleton, D. M., Adsorption behaviour of sulfur containing polymers to gold surfaces using QCM-D. *Soft Matter* **2012,** *8* (1), 118-128.
86. Delcroix, M. F.; Demoustier-Champagne, S.; Dupont-Gillain, C. C., Quartz Crystal Microbalance Study of Ionic Strength and pH-Dependent Polymer Conformation and Protein Adsorption/Desorption on PAA, PEO, and Mixed PEO/PAA Brushes. *Langmuir* **2014,** *30* (1), 268-277.
87. Hu, Y.; Jin, J.; Han, Y.; Yin, J.; Jiang, W.; Liang, H., Study of fibrinogen adsorption on poly(ethylene glycol)-modified surfaces using a quartz crystal microbalance with dissipation and a dual polarization interferometry. *RSC Adv.* **2014,** *4* (15), 7716-7724.
88. Inoue, Y.; Nakanishi, T.; Ishihara, K., Adhesion force of proteins against hydrophilic polymer brush surfaces. *React.Funct. Polym.* **2011,** *71* (3), 350-355.
89. Sharma, S.; Johnson, R. W.; Desai, T. A., Ultrathin poly(ethylene glycol) films for silicon-based microdevices. *Appl. Surf. Sci.* **2003,** *206* (1–4), 218-229.
90. Lundberg, P.; Bruin, A.; Klijnstra, J. W.; Nyström, A. M.; Johansson, M.; Malkoch, M.; Hult, A., Poly(ethylene glycol)-Based Thiol-ene Hydrogel Coatings−Curing Chemistry, Aqueous Stability, and Potential Marine Antifouling Applications. *ACS Appl. Mat. Inter.* **2010,** *2* (3), 903-912.
91. Carter, D. C.; Ho, J. X., Structure of Serum Albumin. *Adv. Prot. Chem.* **1994,** *45*, 153-203.